

International Conference on Space Optics—ICSO 2018

Chania, Greece

9–12 October 2018

Edited by Zoran Sodnik, Nikos Karafolas, and Bruno Cugny



A steep bandpass interference filter with FWHM 11nm centered at 1254nm for studying Lyman Alpha signatures of highly redshifted galaxies

A. Hull

U. Brauneck

J. Gallego

N. Cardiel

et al.



A steep bandpass interference filter with FWHM 11nm centered at 1254nm for studying Lyman Alpha signatures of highly redshifted galaxies

A. Hull^{a,b}, U. Brauneck^{*c}, J. Gallego^d, N. Cardiel^d, C. Cabello^d, R. Guzmán^e, J. M. Rodríguez-Espinosa^f, A. Herrero^f, M. Mas-Hesse^f, E. Salvador^g, A. Manrique^g, A. Marín-Franch^h
^aUniversity of New Mexico, Albuquerque, NM, USA, ^bKendrick Aerospace Consulting LLC, Lafayette, CO, USA, ^cSchott Suisse S.A., Yverdon-les-Bains, Switzerland ^dUniversidad Complutense de Madrid, ^eUniversity of Florida, ^fInstituto de Astrofísica de Canarias, ^gCentro de Astrobiología, ^hUniversity of Barcelona, ^{*}Centro de Física del Cosmos de Aragón (CEFCA)

ABSTRACT

The presented new 1% narrowband filter centered at 1254nm with a FWHM of 11nm required and achieved excellent maximum transmission and deep out of band blocking. Magnetron sputtering was used for the filter coating process. The filter was used in the fully cryogenic near-infrared camera CIRCE of the Gran Telescopio Canarias (GTC) Telescope. The goal of the project is to detect very distant galaxies at the dawn of the Universe. These remote and extremely faint galaxies are selected by their Ly-alpha emission. We report on the spectral and interferometric results of the filter, and provide the spectacular first deep image taken with the 10.4m GTC telescope.

Keywords: optical filter, interference filter, astronomy, instrumentation, narrow bandpass filter, wavefront error

1. INTRODUCTION

The presented filter was produced for the Canarias InfraRed Camera Experiment (CIRCE) which is a near-infrared camera designed and constructed by the University of Florida and is used as a visitor instrument at GTC. The detector is an engineering grade HAWAII-2RG optimized to work on the 1-2.5 micron wavelengths range and has 2048 x 2048 pixels. It covers a field of view of 3.4' x 3.4' with plate scale of 0.1"/pix. It is subdivided into 32 independent channels for quick readout. The CIRCE system gain is 5.3 ± 0.5 e-/ADU and the read noise is ~ 30 -45 e- RMS (channel dependent). The ALBA team is actively following two parallel efforts: (1) the observational detection of high-z Lyman Alpha Emitters (LAE) and (2) An Analytic Model of Intergalactic-medium and GALaxy (AMIGA) evolution since the dark ages previous to reionization. Although in 2014 Planck mission predicted one single re-ionization at $z=11.3 \pm 1.1$, AMIGA predictions are that it is very likely that the reionization occurred in two stages: a first one at $z \sim 10$ due to Pop. III stars, whose formation ended at this epoch as molecular cooling was quenched, and a second and definitive one at $z \sim 6$, due to young galaxies formed at $z > 6$. We search LAEs at $z \sim 9.3$ in order to find observational proofs to confirm or not this scenario. Comparison with J band fluxes allow us to select those targets with a flux excess in the Narrow-Band filter presented in this paper with respect to the Broad-band filter. If the target is at $z= 9.3$, it will be a dropout in all photometric bands bluer than J. Once we have rejected lower-z contaminants, accurate photometry in the narrow band filter will provide us with the Ly α luminosity and equivalent width. Number densities of LAE's will be compared with theoretical predictions to confirm or reject the double reionization scenario. The filter has been selected to coincide with a region which avoids OH emissions and atmosphere absorptions and lies in a wavelength range with minimum sky continuum emission, leading to discrete redshift values.

We have obtained the deep image (displayed in Figure 1 Right) and achieve to improve the ratio S/N and to be able to see some fainter objects. We have an image with a total exposure time around 16500s. Although the final image exhibits cosmetic defects, specially at the borders, an important fraction of the image area is useful for our scientific purposes. We identified the objects comparing our final image with the HST/WFC3 image of AEGIS-16 (Figure 1 Left). Figure 2 shows the identified objects type galaxy in color mosaic of HST (left: with filters optical V band 555nm and pseudogreen V+I bands, infrared I band 814nm and right: object in CIRCE image (filter presented here). The image was

smoothed applying a median filter in order to observe better the objects. Orientation: North is 218° right of the vertical. Box size: 8 arcsec x 8 arcsec. The first results are summarized in [1].

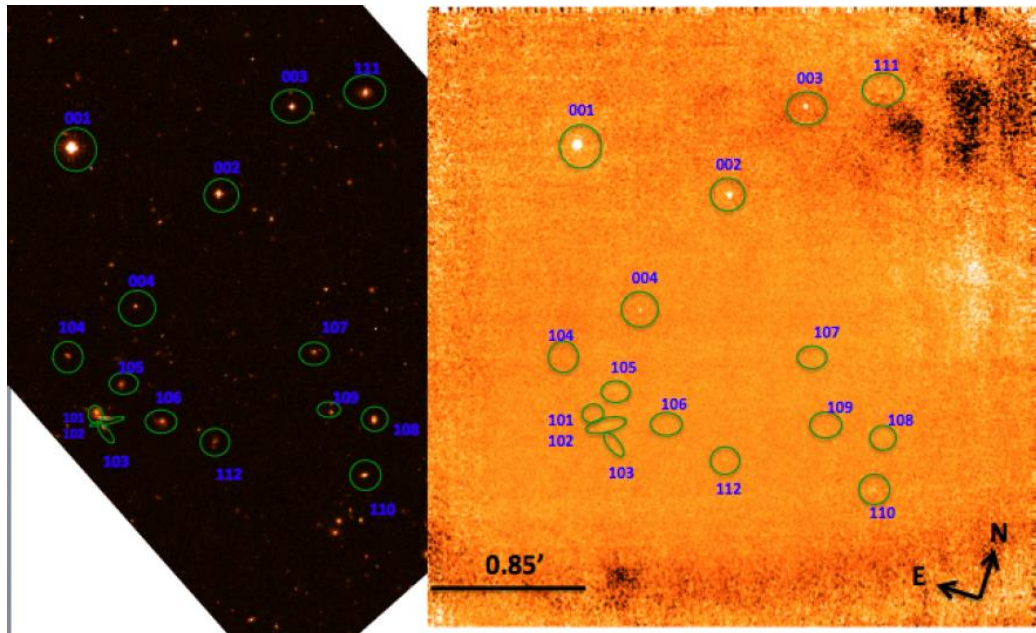


Fig. 1 region of observation. We identify 16 objects in the HST/WFC3 image (F125W filter, exposure time of 81028.46s) of AEGIS-16 (left), and in the same way, in our CIRCE deep image (presented narrowband filter, exposure time of 16500s) (right).

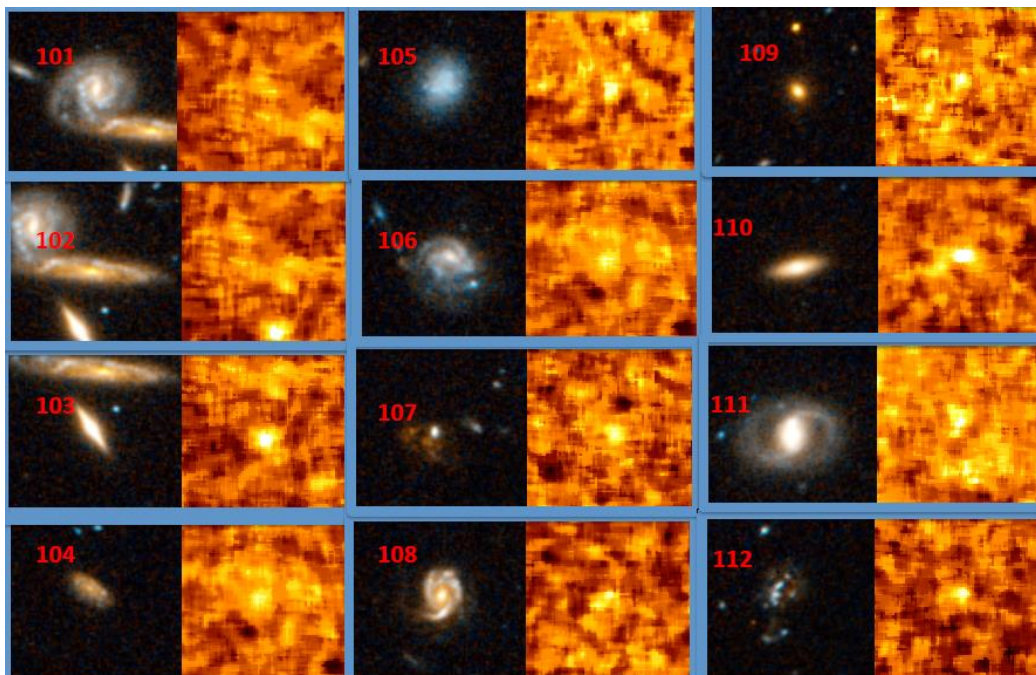


Fig. 2 Identified objects type galaxy (See Table 3.6) . Left: object in color mosaic of HST (Filters: optical V band (555 nm) and pseudogreen V+I bands, Infrared I band (814 nm)). Right: object in CIRCE image (Filter: ALBA Narrow Band). The image was smoothed applying a median filter in order to observe better the objects. Orientation: North is 218_ right of the vertical. Box size: 8 arcsec × 8 arcsec

A color-color diagram is shown in Figure 3. In the plot we observe that the object 105 has also the most blue color of our list of candidates, followed by the object 106. The red colors may be attributed to dust, although older stellar populations have similarly red colors. The elliptical galaxies (objects 109 and 110) present red colors as expected. The object 102 presents red color too (although it is not an elliptical galaxy) due to dust in the disk. The results are in good agreement with the observed colors in the color-mosaic of HST. The objects in the top left of the diagram correspond with quiescent galaxies, without young stellar population. We want to highlight that we have two possible interlopers detected in our narrowband filter: the object 107 is a possible H α emitter at $z_{\text{spec}}=1.01$ and the object 112 is a possible [OIII] emitter at $z_{\text{phot}}=1.53$.

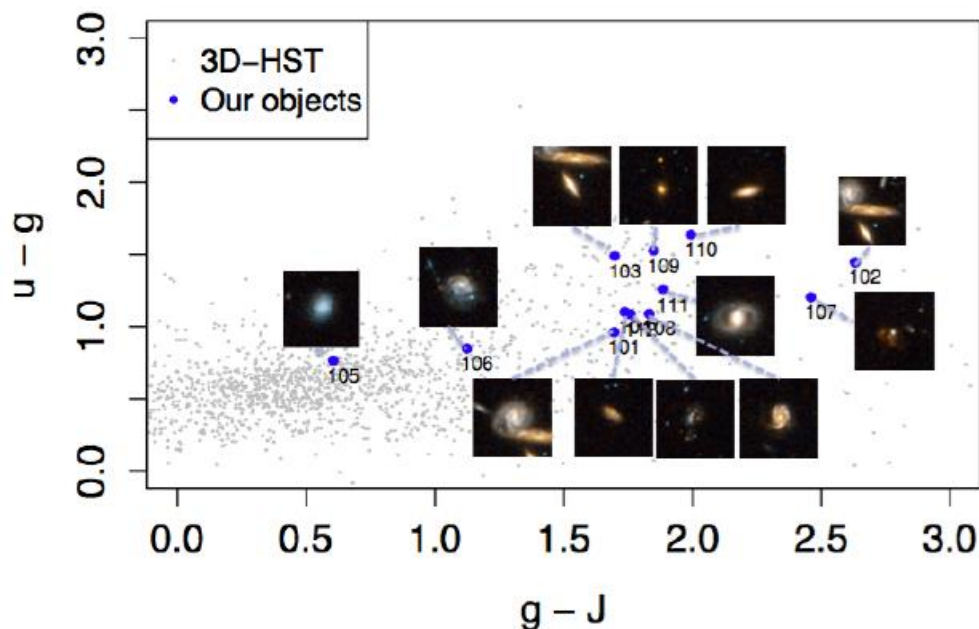


Fig. 3 Rest-frame ugJ diagram of the galaxies of AEGIS-16 3D-HST (gray) and our identified galaxies (blue). Data obtained from AEGIS 3D-HST data release v4.1.

2. DESIGN AND PRODUCTION OF THE CIRCE NARROW BAND FILTER

2.1. Design of the interference filter

The design principle of the filter is a double sided coating on a fused silica Corning 7980 grade 1F substrate. On the first side of the substrate the coating has been designed as a 5-cavity Fabry-Perot (FP) bandpass design with 82 alternating layers of Nb₂O₅ and SiO₂. The basic building blocks of the FP-design are classical third and fourth order dielectric mirrors and first and second order resonator layers with high refractive index layers in Nb₂O₅:

$$(HL)^3 4H (LH)^3 L (HL)^4 2H (LH)^4 L (HL)^4 4H (LH)^4 L (HL)^4 2H (LH)^4 L (HL)^3 4H (LH)^3 L$$

With H: quarter wave optical thickness Nb₂O₅ and L: quarter wave optical thickness SiO₂

To tune the full width at half maximum (FWHM) of the filter to 11nm selected mirror layers were modified to 3 quarter wave thickness layers. The nominal central wavelength is 1254nm. For a good antireflection of the filter's passband, the thickness of the last 2 layers was optimized for maximum transmission in the passband. Figure 4 shows the theoretical design of the 5-cavity bandpass with FWHM 10.35nm for collimated light at an angle of incidence perpendicular to the filter surface.

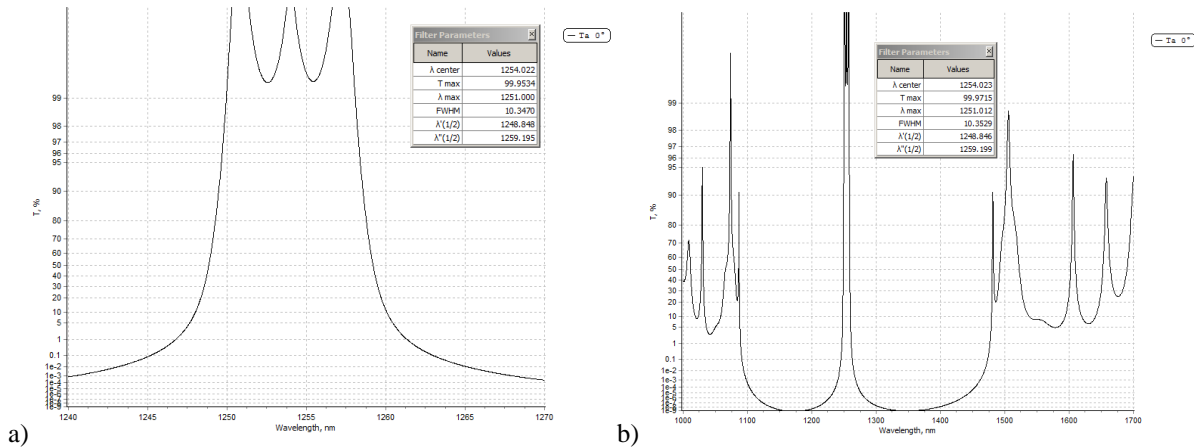


Fig. 4 a) and b) show the calculated design curve of the bandpass coating on the first side of the substrate. The full width at half maximum of the theoretical design is 10.35nm and the slope is 1.69nm from T=5% to T=80%.

A blocking filter was coated on the second side of the substrate to achieve a blocking of optical density 5 ($T=10^{-5}$) in the range 1050-1650nm. This coating was also designed by the Fabry-Perot principle with 13 coupled resonators and 52 layers:

$$(H\ 2L\ HL)^3\ (H\ 4L\ HL)\ (H\ 2L\ HL)^5\ (H\ 4L\ HL)\ (H\ 2L\ HL)^3\ @\ \text{nominal design wavelength } 1254\text{nm}$$

With H: quarter wave optical thickness Nb_2O_5 and L: quarter wave optical thickness SiO_2

The thicknesses of the last two layers of the blocking filter were optimized for maximum transmission of the filter in the passband of the bandpass. Figure 5 shows the theoretical transmission curve of the blocking filter (black solid curve) and the theoretical transmission curve of the bandpass coating (brown discontinued curve).

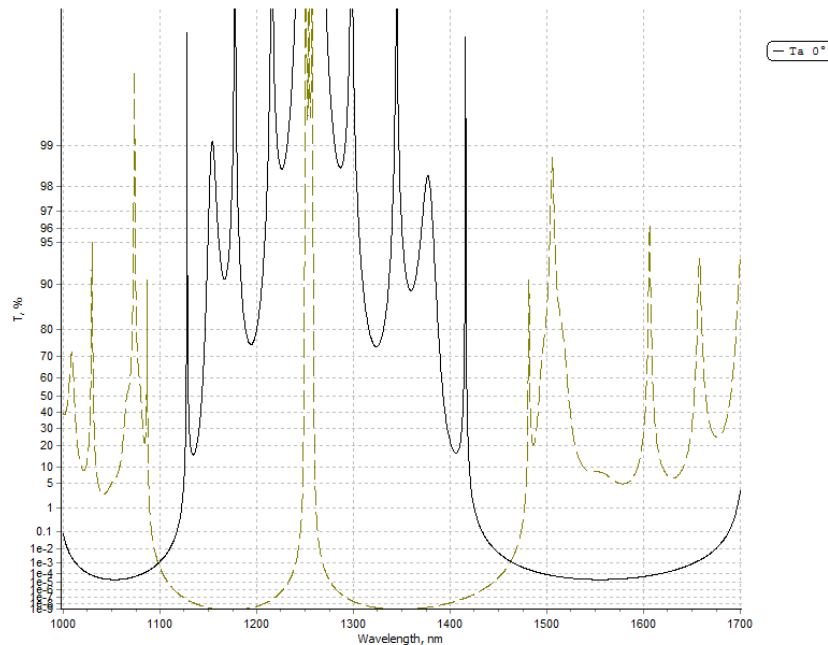


Fig. 5 shows the calculated design curve of the blockfilter coating on the second side of the substrate (black curve) and the theoretical design of the narrow bandpass on the first side (brown discontinued curve).

2.2. Production of the bandpass filter

The deposition technique of the two filter layers systems have been chosen to be plasma assisted reactive magnetron sputtering (PARMS). The PARMS 0 process results in very dense and humidity resistant coatings with a very low temperature shift. Similar filters were measured to have a temperature shift from room temperature to 77°K of -0.125% of the central wavelength, which accounts for 1254nm to a shift of -1.57 nm. This temperature shift was taken into account at the centering of the filter during its production. The mechanical and environmental resistance of the coatings are excellent due to the high density of the metal oxide films. The coatings resist cleaning with alcohol or acetone.

The coating process stability and particularly the thickness monitoring is of highest importance for the production of high quality bandpass filters during the coating process. In production practice a combination of direct monochromatic [3] and rotation monitoring was proven to be very accurate and reproducible. The direct monochromatic transmission monitoring provides a self-compensation of layer thickness errors, when the quarterwave optical thickness layers are terminated always in the maximum or minimum points of the transmission measured at the centerwavelength of the Fabry-Perot filter. Thereby, should a previous layer be too thick or too thin, the next layer which is stopped again at the next extremum of the transmission will partly compensate for the thickness error and only a small fraction of the transmission of the filter in central wavelength, that corresponds to the optical thickness error is lost. Usually this error is only in the order of magnitude of tenths of a percent or even lower. For the so-called rotation-monitoring, the number of rotations of the substrate holder was monitored, which was calibrated by the optical thickness increase per rotation in previous layers, that were monitored optically by measuring the transmission change during the layer growth. By this method, we insure a very accurate *insitu*-measurement of the actual thickness. A substrate rotation of 180 rpm and a resulting high rate of data sampling result in a very accurate thickness monitoring and tangential uniformity in the sense of rotation. The radial uniformity of the center wavelength of the filters was tuned by distribution shields and magnetic field tuning of the magnetron sputter sources.

It is also possible to deposit an AR-coating on the entrance side of a substrate and a bandpass coating with deep and wide blocking on the backside to achieve a similar spectral behaviour. In practice however this solution that requires more than 130 layers in a single coating has the tendency to show more oscillations of transmission in the passband of a filter. Furthermore if the bandpass coating and a blocking coating can be deposited independently on two sides of a component the spacial uniformity of the bandpass is generally much better in control. The bandpass coating on one side can be optimized for uniformity of centralwavelength and FWHM and the blocking coating can be optimized for high transmission, low ripple and high rejection. These were the main considerations for the choice of the current filter layer designs.

The important criteria for the choice of substrate types were high transmission, low climatic sensitivity, low autofluorescence and good behaviour in the polishing process.

2.3. Bandpass filter specification

The fused silica substrates (7980 grade 1F) with a diameter 68.0mm +/- 0.1mm and thickness 6.0mm +/- 0.1mm were polished to P3 quality the transmitted wavefront should be smaller than $\lambda/4$ @ 633nm over the clear aperture 65mm and smaller than $\lambda/8$ @ 633nm in every subaperture 25x25mm. The surface defects were specified by scratch-dig 60/40 per MIL 13830B and the parallelity should be smaller than 30 arcsec. To accomplish that, the double sided polishing was applied at SCHOTT Suisse S.A..

At an angle of incidence of 2.2° the bandpass should be centered at 1254 +/-2nm taking the temperature shift and angular shift into account. The maximum transmission should be higher than 90% and the out of band blocking should be 10-5 average (OD5) from 1050-1650nm. The uniformity of the central wavelength, measured by a 5-point measurement (center point and 4 points about 5-10mm from the edge should be +/-2nm. The peak transmittance uniformity commonly named "passband ripple" should be smaller than 5% peak-to-valley and the peak transmittance flatness defined by the difference between minimum and maximum value within the passband should be smaller than 5%. The Full-width-half-maximum (FWHM) was specified by 11.0 +/- 0.5 nm. The slope of the rising and falling edges should be better than 0.135% evaluated as $|\lambda@80\% - \lambda@5\%|/CWL$.

3. MEASUREMENTS OF NARROW BANDPASS FILTER

The substrate as well as the coatings for this narrow bandpass CIRCE filter was entirely produced at SCHOTT SUISSE S.A. Yverdon-les-Bains, Switzerland. The complete process from the design of the filters to final measurement was under control and responsibility of SCHOTT. Measurement results for the transmittance/reflectance of the filters as well as the transmitted wavefront measurements are presented.

3.1. Transmission measurement results

Spectral transmission measurements were performed on a Agilent CARY 5000. The measurement was performed with a data interval 0.1nm, scan rate 60nm/min, averaging time 0.1sec, slit bandwidth 0.2nm, aperture half-angle 7.5° , angle of incidence 2.2° with background and zero-correction at room temperature (21°C). The spectral uniformity was measured by a 5-point measurement (center + 4 corner points). Due to the lateral extension of the probe beam the lateral measurement points of the filter were chosen at approximately 5-10 mm distance from the edge. As shown in Fig. 6, the specified maximum transmission was exceeded.

A wavelength offset from the measurement conditions to a collimated beam was taken into account with +0.4nm. So the target centering was derived from the measurement offset of +0.4nm and the thermal wavelength shift of +1.57 nm. This leads to a target centering of the bandpass of 1256.97 nm.

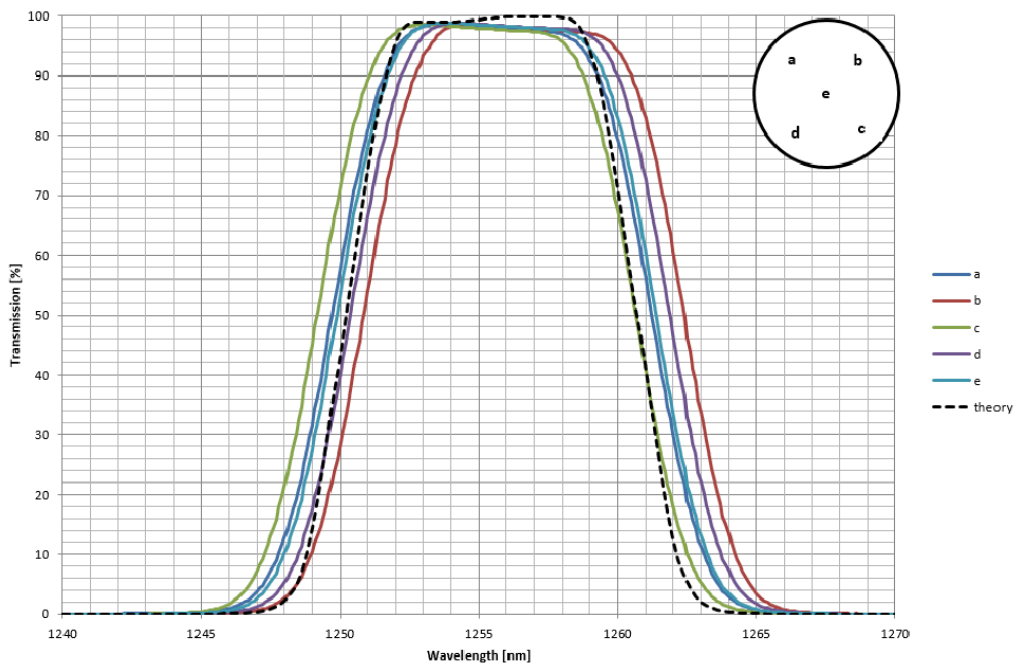


Fig.6 transmission measurement performed on 5 points of the filter (see insert right upper corner). The discontinued curve shows the theoretical filter curve calculated for the aperture half-angle of 7.5° in the photospectrometer used and an incident angle of 2.2° specified for the application.

The uniformity of the filter was evaluated from the measurements. In Table 1 the characteristic values of the measurement in Fig. 6 are displayed. The central wavelength (cwl) uniformity of the filter is 0.14% and the variation of the maximum transmission over the 5 points is only 0.33%. The FWHM shows a variation that is close to the specified resolution of 0.2 nm of the Agilent CARY 5000 instrument in the NIR.

	a	b	c	d	e	uniformity
CWL	1255.46	1256.62	1254.92	1256.13	1255.63	0.14%
FWHM	11.57	11.59	11.54	11.55	11.53	0.52%
Tmax	98.55	98.59	98.53	98.83	98.85	0.33%

Table 1 evaluation of the characteristic values of the 5 point measurement shown in Fig.6

The out of band blocking from 1050-1650nm is better than the specification OD5 ($T < 10^{-5}$) on average as demonstrated by measurements shown in Fig.7 . The average value of blocking between 1050 nm and the shortwave 1%-footpoint of the bandpass is 6.34 OD-units. The longwave blocking value between the longwave 1%-footpoint of the bandpass region and 1650nm is 6.62 OD-units. The measurements were performed with state-of-the-art photometers Agilent CARY5000 that have a very good dynamic range of their detectors to resolve a blocking of OD7 in certain wavelength ranges. The blocking measurements were carried out with reference beam attenuation. The measurement parameters for the blocking measurement were interval 3nm, scan rate 360nm/min, averaging time 0.5 seconds, slit bandwidth 3 nm, aperture half-angle 7,5° and angle of incidence 0° with background and zero-correction at room temperature (21°C).

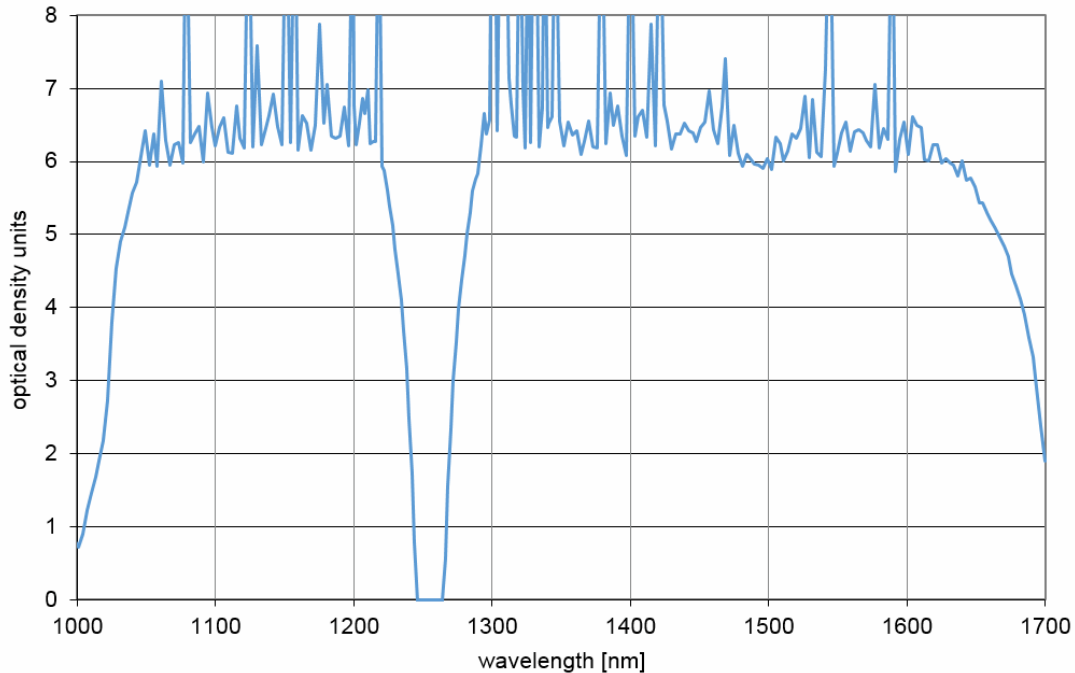


Fig.7 blocking measurement performed with an Agilent Cary 5000 with reference beam attenuation showing an average blocking from 1050-1650nm of better than OD 6.

3.2. Measurement result of the transmitted wavefront error

The transmitted wavefront was measured with a Zygo XPZ interferometer on the clear aperture of 65 mm diameter and shows a distortion of 0.01 wave evaluated with the reference wavelength 546nm. See Figure 8.

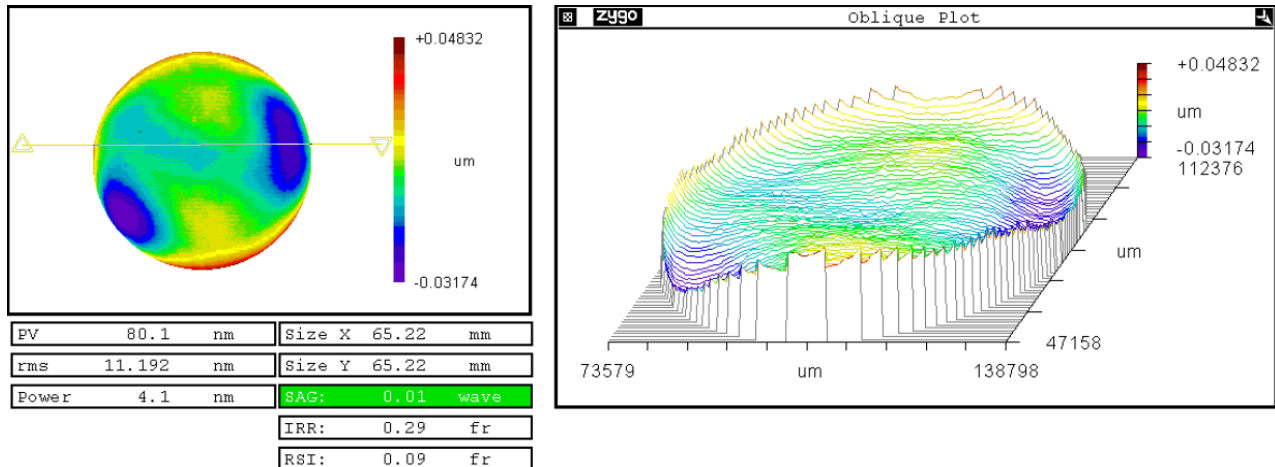


Fig. 8: measurement result of transmitted wavefront evaluated according to DIN ISO 10110 (ref. wavelength 546nm) to be 13/0.01(0.29/0.09).

The local transmitted wavefront was evaluated in all subapertures of 25x25mm on the clear aperture and the worst distorted spot was evaluated to have a sagittal error of 0.02 waves @ 546nm (see Fig. 9). As conclusion the filters exceed the global and local specification of transmitted wavefront distortion. Finally the parallelity of the filter was measured to be 5 arcseconds.

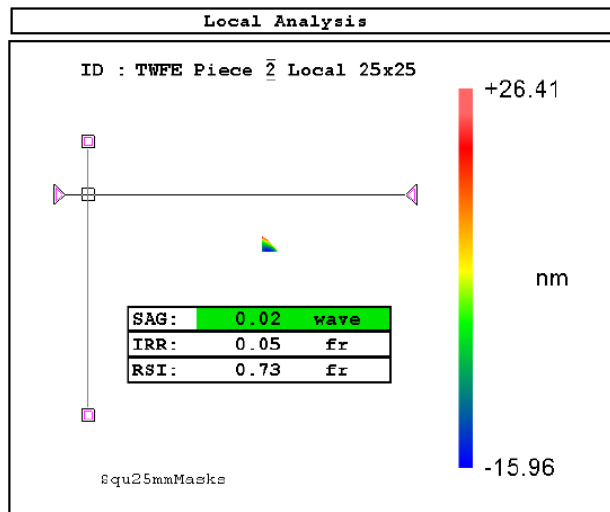


Fig. 9: measurement result of transmitted wavefront in all local subapertures 25x25mm.

4. SUMMARY

We report on an ultradeep NIR- image taken with the fully cryogenic camera CIRCE of the Gran Telescopio Canarias Telescope. For that purpose Schott Suisse S.A. produced a steep near infrared interference bandpass filter with a central wavelength of 1254 nm on a fused silica substrate. The detailed specification of the filter is given and we describe the filter design and the coating process by using the PARMS magnetron sputtering technology. The filter achieved excellent maximum transmission of nearly 99% and a spectral uniformity of 0.14% over the clear aperture of 65mm with blocking better than OD6 from 1050 – 1650nm. The interferometric measurements show a transmitted wavefront distortion of 0.01 waves @ 546nm over the clear aperture which guaranties best image quality in the performed scientific observations.

ACKNOWLEDGEMENT

We acknowledge financial support from the Spanish Ministry of Economy and Competitiveness (MINECO) under grant number AYA2016-75808-R, which is partly funded by the European Regional Development Fund (ERDF) and Convocatoria de ayudas para la contratación de investigadores [predoctorales or postdoctorales] program, which is partly funded by European Social Fund.

REFERENCES

- [1] Cristina Cabello Gonzalez, «observational test of a double reionization scenario by detecting galaxies at very high z with the GTC», master thesis, Universidad Complutense de Madrid, Facultad de Ciencias Fisicas, Sept. 2017
- [2] Scherer, M. et al., "Innovative production of high quality optical coatings for applications in optics and optoelectronics," 47th annual technical conference proc. of the society of vacuum coaters, 179, (2004).
- [3] MacLeod, H. A., "Turning value monitoring of narrow-band all-dielectric thin-film optical filters," Optica Acta, International Journal of Optics 19, 1-28, (1972).